Association of a Mutation in TRPV3 with Defective Hair Growth in Rodents

Makoto Asakawa[1,4], Takeshi Yoshioka[1,4], Takaji Matsutani[2], Ichiro Hikita[1], Minoru Suzuki[1], Itsuki Oshima[1], Kiyoshi Tsukahara[1], Akinori Arimura[1], Tatsuya Horikawa[3], Tsutomu Hirasawa[1] and Tsuneaki Sakata[1]

DS-*Nh* mice and WBN/Kob-*Ht* rats are spontaneous hairless mutant rodent strains. These animals develop spontaneous dermatitis under normal conditions. The non-hair *Nh* and *Ht* phenotypes are inherited in an autosomal dominant fashion, and the *Nh* mutation possesses a high potency for penetration. We previously reported that genes involved in dermatitis and hairlessness did not segregate from each other. Here, we carried out genetic analysis to identify the genes responsible for these hairless mutations. An amino-acid substitution at the same position in one gene was detected in DS-*Nh* mice and WBN/Kob-*Ht* rats: Gly573 to Ser (*Nh* mutation) or Gly573 to Cys (*Ht* mutation), located in the transient receptor potential (TRP) cation channel subfamily V member 3 (TRPV3) gene. Mutated TRPV3 was expressed in skin keratinocytes of DS-*Nh* mice. Histopathological analyses revealed that mast cells in skin lesions were increased in both rodents compared to their age-matched parent strains, and that this may partially be due to hairlessness and dermatitis. We concluded that TRPV3 was the gene responsible for *Nh* and *Ht* mutations, and that mutation in TRPV3 possibly correlated with increased mast cell numbers.

Journal of Investigative Dermatology (2006) **126,** 2664–2672. doi:10.1038/sj.jid.5700468; published online 20 July 2006

INTRODUCTION

Several hairless mutants of rodents have been reported, and many of these involve mutations that are inherited in an autosomal recessive fashion (Zhang *et al.*, 2005). On the contrary, the mouse *Nh* non-hair phenotype is inherited in an autosomal dominant fashion (Watanabe *et al.*, 2003). We think that it is easy to introduce the phenotype of this mutation to another strain of mice using simple breeding methods, enabling us to detect the location of this gene. Furthermore, we can analyze this mutation in many kinds of mice that have their own genetic background. The DS-*Nh* mice used in this study were derived from a colony of DS strain inbred in 1976. DS mice were developed in 1954 from an outbreed of a stock from the Central Institute for Experimental Animals, Tokyo, Japan. DS and DS-*Nh* mice have been maintained at Aburahi Laboratories, Shionogi & Co., Ltd, Shiga, Japan. Recently, we reported that WBN/Kob-*Ht* rats, which are also spontaneous hairless mutants with an autosomal dominant inheritance mode of the *Ht* mutation (Akimoto *et al.*, 2000), developed atopic dermatitis (AD)-like dermatitis (Asakawa *et al.*, 2005). It was interesting that both these rodents developed AD-like dermatitis spontaneously, but only when they were raised in the presence of *Staphylococcus aureus* and not under SPF (*S. aureus*-free) conditions. This spontaneous dermatitis in both rodents had very similar characteristics including the following (Haraguchi *et al.*, 1997; Hikita *et al.*, 2002; Yoshioka *et al.*, 2003; Asakawa *et al.*, 2005): (1) *S. aureus* could be isolated from skin lesions, (2) serum levels of IgE and IL-4 were significantly increased, (3) numbers of whole mast cells and CD4-bearing T cells were significantly increased, and (4) hyperkeratosis was detected in skin lesion with dermatitis. Furthermore, the *Nh* locus was mapped on mouse chromosome 11 (Watanabe *et al.*, 2003), and the *Ht* locus on rat chromosome 10 (Akimoto *et al.*, 2000), and both loci are located in contiguity with the linkage site.

In this report, we describe breeding studies involving DS-*Nh* mice, and the positional cloning of the responsible gene for the *Nh* mutation. Our breeding studies indicated that the genes involved in dermatitis and hairlessness were very tightly linked, and did not segregate from each other. In genetic studies, we identified one amino-acid substitution (Gly573 to Ser) in the transient receptor potential (TRP) cation channel subfamily V member 3 (TRPV3) of DS-*Nh* mice. In addition, one amino-acid substitution of the same type (Gly573 to Cys) was detected in WBN/Kob-*Ht* rats. Therefore, these mutations in TRPV3 appeared to correlate with *Nh* and *Ht* mutations.

[1]*Shionogi Discovery Research Laboratories, Shionogi & Co., Ltd, Osaka, Japan;* [2]*Division of Immunology and Embryology, Department of Cell Biology, Tohoku University School of Medicine, Sendai, Japan and* [3]*Division of Dermatology, Department of Clinical Molecular Medicine, Kobe University Graduate School of Medicine, Kobe, Japan*

[4]*These authors contributed equally to this work.*

Correspondence: Dr Tsuneaki Sakata, Shionogi Discovery Research Laboratories, Shionogi & Co., Ltd, Futaba, Toyonaka, Osaka 561-0825, Japan. E-mail: takeshi.yoshioka@shionogi.co.jp

Abbreviations: AD, atopic dermatitis; 2-APB, 2-aminoethoxydiphenyl borate; BAC, bacterial artificial chromosome; NGF, nerve growth factor; TRP, transient receptor potential; TRPV3, TRP cation channel subfamily V member 3

Received 12 January 2006; revised 16 May 2006; accepted 23 May 2006; published online 20 July 2006

Numbers of skin mast cells were significantly increased in DS-*Nh* mice and WBN/Kob-*Ht* rats compared to those in their parent strains (Figure 5b). Traditionally, mast cells are known to be directly involved in allergic and inflammatory processes (Weber *et al.*, 1995; Galli *et al.*, 2005). For example, repeated application of allergen induced an increase in the number of mast cells (Mitchell *et al.*, 1986) and histopathological studies indicated that mast cells infiltrated to the skin lesion in patients with AD (Piloto *et al.*, 1990). However, increasing evidence supports particular roles for mast cells in mechanisms controlling tissue remodeling (Irani *et al.*, 1992; Levi-Schaffer, 1995; Kendall *et al.*, 1997) such as cyclic growth and the regression phase of mouse hair follicles (Maurer *et al.*, 1997). Hair follicles go through alternating periods of growth, regression, and quiescence (anagenesis, catagenesis, and telogenesis), and thus hair cycles are involved in the development of hairlessness in humans and rodents. Furthermore, mast cells have the highest potency for containing histamine (Enerback and Wingren, 1980), and the temporary increase in histamine contents in skin is important for normal hair growth in mice (Hamada and Suzuki, 1996). In fact, an increasing number of mast cells is a prominent feature in patients with male pattern alopecia (Lattanand and Johnson, 1975). Considering these results, *Nh* and *Ht* mutations may cause an increase in mast cells at a skin lesion, and this proliferation may be associated with both phenotypes of hairlessness and the development of dermatitis.

This paper reports the elucidation of clinical roles for TRPV3 *in vivo*. Our results indicated that a mutation in *TRPV3* caused hair loss and might also cause AD-like dermatitis in DS-*Nh* mice and WBN/Kob-*Ht* rats. We believe that TRPV3 might become a therapeutics target for certain types of alopecia and dermatitis, such that agonists and/or antagonists of TRPV3 may become therapeutic tools for these pathologic conditions.

RESULTS

Breeding studies

DS-*Nh* (*Nh/Nh*) mice were mated with DS, BALB/c, or C57BL/6 mice. Phenotype segregations in N1 generation (DS-*Nh* × DS, BALB/c, or C57BL/6) and N2 generation mice (F1 mice × DS, BALB/c, or C57BL/6) were analyzed according to phenotype (data not shown), and all hairless mice developed dermatitis. Expected ratios of phenotype segregations are shown in Figure 1a. Detailed observations of the characteristics of about 1,000 F1 and/or N2 mice indicated that the hairless and dermatitis phenotypes did not segregate from each other. In Figure 1, we present clinical features of N2 generation mice at 5 weeks (b) and 20 weeks (c) of age.

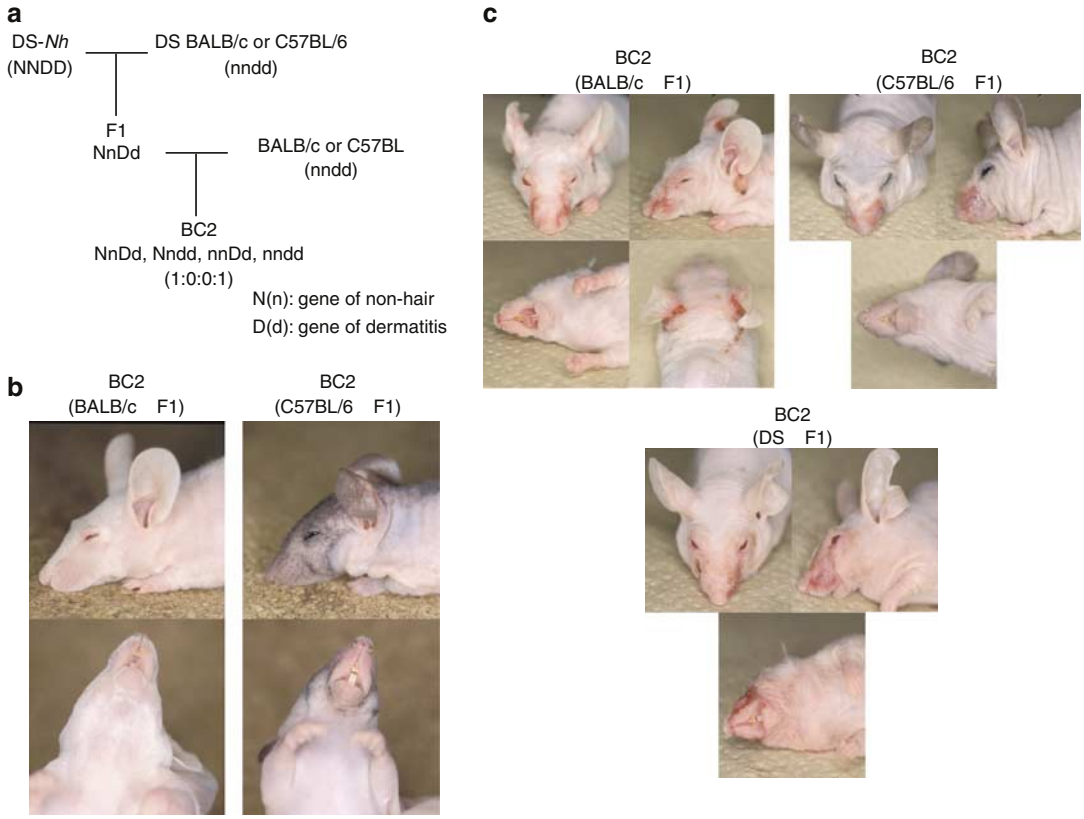

Figure 1. Results of breeding studies. (**a**) Pedigree structure and expected ratios of genotypes. (**b**) Clinical features of BALB/c-*Nh* (*Nh*/+) and C57BL/6-*Nh* (*Nh*/+) mice maintained in an SPF room until 5 weeks old. (**c**) Clinical features of DS-*Nh* (*Nh*/+), BALB/c-*Nh* (*Nh*/+), and C57BL/6-*Nh* (*Nh*/+) mice maintained in a conventional room until 20 weeks old.

Positional cloning of the gene responsible for the *Nh* mutation

To localize precisely the *Nh* locus on mouse chromosome 11, an initial linkage analysis was conducted using DS-*Nh* (*Nh*/+) and NC/Nga mice. As the two strains were genetically distant from each other, we could arrange for many polymorphic DNA markers to determine the chromosomal position of the *Nh* locus. Mice of the first backcross generation were phenotyped by hairlessness, and genotyped using microsatellite markers that were polymorphic between the DS-*Nh* and NC/Nga strains. Briefly, the progenies were categorized into 10 groups according to the presence of chromosome crossover between the genomes of parent mice (Figure 2a), and the hairless phenotype was analyzed. Results indicated that a significant lineage was observed between the *Nh* locus and the marker D11Mit194, but not D11Mit219 and D11Mit352. We concluded that the *Nh* region was located between markers D11Mit219 and D11Mit352 on mouse chromosome 11. Figure 2b shows the known genes located between markers D11Mit219 and D11Mit352 on mouse chromosome 11. We then carried out a detailed sequencing analysis of this genomic region using bacterial artificial chromosome (BAC) libraries prepared from DS and DS-*Nh* mice. Nucleotide sequences of the two strains were carefully compared, and a gene mutation was detected in *TRPV3*. Mutation of G1717A (Figure 3a) caused an amino-acid alteration of Gly573 to Ser (Figure 3b) in DS-*Nh* mice. This mutation represented a significant gene mutation in our sequencing analysis.

To confirm whether *TRPV3* was also mutated in WBN/Kob-*Ht* rats, we sequenced the entire coding regions of *TRPV3* in these rats and the parent strain WBN/Kob. We found that there was a gene mutation at the same position (G1717T) in WBN/Kob-*Ht* rats, which caused an amino-acid alteration from Gly573 to Cys (Figure 3b), as in DS-*Nh* mice. Figure 3c shows the predicted structure of TRPV3, and the locations of the *Nh* and *Ht* mutations are indicated with red circles.

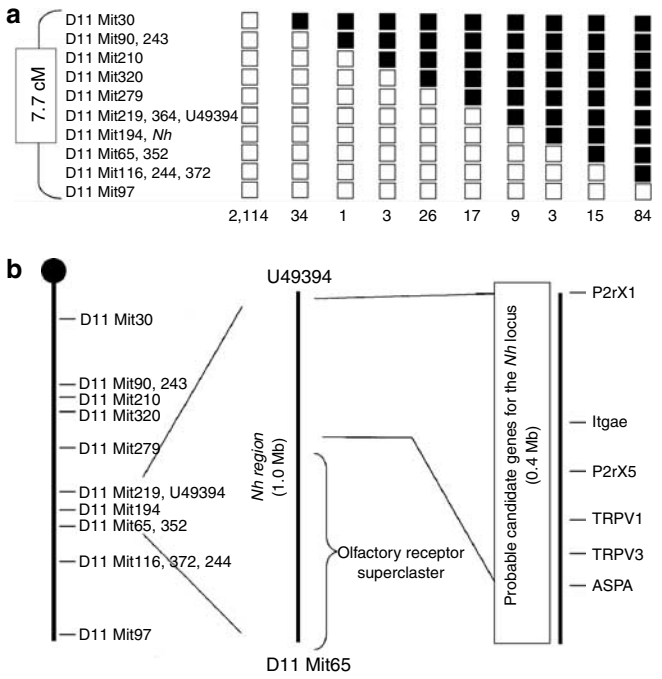

Figure 2. High-resolution linkage and physical maps of the *Nh* region. (**a**) Genotyping data using polymorphic markers in 2,303 animals from (DS-*Nh* × NC/Nga) F1 × NC/Nga backcross excluding unlinked regions from the *Nh* locus in chromosome 11. Each box represents a frame format of genetic markers. The boundary between black boxes and white boxes shows the autosomal region of chromosomal crossover. (**b**) The *Nh* locus is linked to marker D11Mit194 but not to markers U49394 and D11Mit65. The physical interval for the *Nh* region delimited by markers U49394 and D11Mit65 is about 1 Mb. Coding regions in this interval were completely sequenced in DS and DS-*Nh* mice. Furthermore, non-coding regions of the probable candidate genes for the *Nh* locus were also sequenced in DS and DS-*Nh* mice. The six known genes in this figure are listed in the NCBI databases, and include the candidate gene TRPV3. Relative distances of these genes are reflected on a real scale in the genome.

Expression of TRPV3 in mouse skin

As the DS-*Nh* strain was maintained by breeding *Nh*/+ males with +/+ females, all DS-*Nh* mice used in this study were heterozygotes (*Nh*/+). To investigate the site of expression of *TRPV3* with the *Nh* mutation, we carried out Northern and *in situ* hybridizations using mRNA and skin tissues from DS-*Nh* mice (Figure 4a). Northern hybridization showed that *TRPV3* was abundantly expressed in skin tissues. *In situ* hybridization revealed that TRPV3 was expressed in skin keratinocytes (Figure 4b). Next, we carried out Western blot hybridization using proteins prepared from primary skin keratinocytes, which were obtained from DS and DS-*Nh* mice, and an anti-TRPV3 polyclonal antibody. TRPV3 protein was detected in skin keratinocytes (Figure 4c). We also estimated expression ratio of the TRPV3 gene with or without *Nh* mutation in DS-*Nh* mice (heterozygotes), using a PCR-restriction fragment length polymorphism method (Figure 4d). We could detect 52 and 131 base restriction fragments in DS-*Nh* mice and so could roughly estimate the quantity of TRPV3 with the *Nh* mutation using both bands. As the size-related intensity of the DNA fragments is significantly correlated with their amounts, we could use densitometric methods to estimate the amounts from the intensity of these bands and information of their size (data not shown). In general, the mutated TRPV3 gene was expressed at half the rate of the total gene expression in DS-*Nh* mice.

Pathological changes caused by the *Nh* mutation

To clarify phenotypic influences of the *TRPV3* mutation, we carried out histopathological analysis in skin lesions where the TRPV3 gene was expressed in both rodents with or without the mutation. Histological changes such as an increase in the number of hair follicles were observed in DS-*Nh* mice and WBN/Kob-*Ht* rats kept under SPF conditions at 5 weeks of age (Figure 5). The distance between individual hair follicles and epidermis was not constant in rodents with mutated TRPV3. Next, we stained skin sections from these rodents at 5 weeks of age, using acidic toluidine blue to detect mast cells (Figure 5). In skin lesions where mutated *TRPV3* was expressed, there were significant increases in the

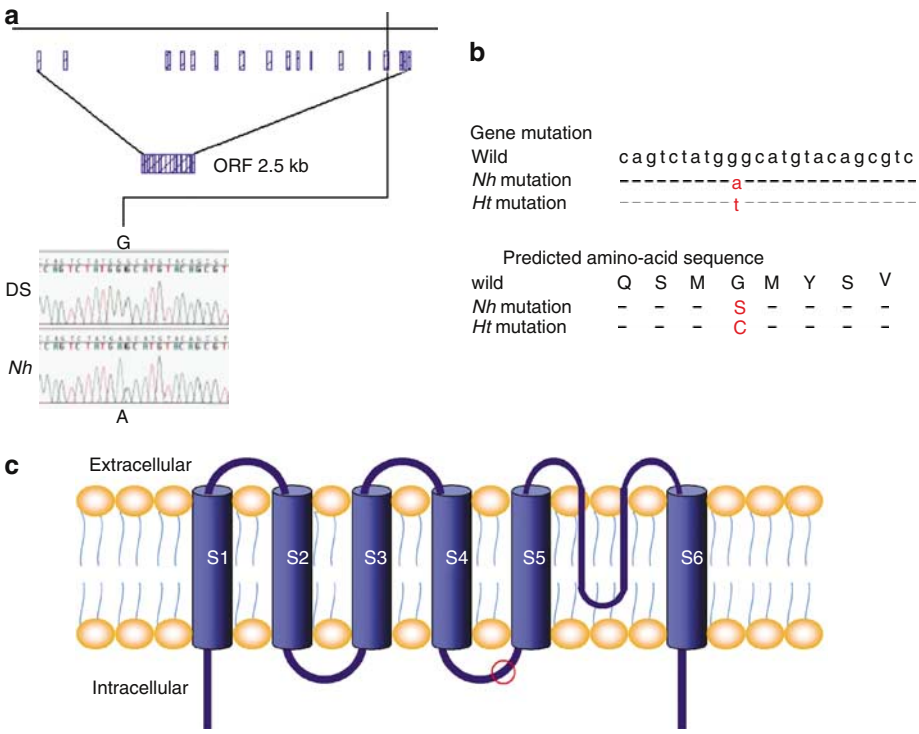

Figure 3. DS-*Nh* mice possess the TRPV3 gene with one point mutation. (**a**) Comparison of the nucleotide sequence of TRPV3 between DS-*Nh* and DS mice. (**b**) Predictions of the amino-acid sequences show the alteration of Gly573 to Ser (*Nh* mutation) and Gly573 to Cys (*Ht* mutation) in TRPV3 of DS-*Nh* mice and WBN/Kob-*Ht* rats, respectively. (**c**) Scheme showing the structure of TRPV3 and position of the alteration (red circle). In this study, we carried out positional cloning to reveal the gene responsible for the *Nh* mutation. Sequencing data for coding and non-coding regions are required in positional cloning methods. In addition, we sequenced the TRPV3 coding region of another mutant animal (WBN/Kob-*Ht* rat), which possesses almost the same phenotypes as DS-*Nh* mice. Details are described in the Discussion section.

number of mast cells. In the lungs and small intestine, no increase in the number of mast cells was observed in DS-*Nh* mice and WBN/Kob-*Ht* rats at 5 weeks of age compared to age-matched DS mice and WBN/Kob rats (data not shown).

Histamine levels in skin lesions of DS and DS-*Nh* mice

As the skin histamine level is known to change after depilation in mice (Hamada and Suzuki, 1996), we measured histamine levels using enzyme-based color developing methods in the skin of DS and DS-*Nh* mice at 0, 1, 2, and 3 weeks of age. The levels of histamine in the skin tissue from DS-*Nh* mice significantly increased compared to those from age-matched DS mice (Figure 6). In DS mice, the levels of histamine were highest just after birth, and the levels were maintained until 3 weeks after birth (Figure 6). In DS-*Nh* mice, the levels of histamine dynamically changed after birth and were highest at 2 weeks after birth (Figure 6). Further, levels of histamine in the skin from both strains at 5 weeks age decreased to an undetectable level in DS mice, and to about 150 nmol/g tissue in DS-*Nh* mice (data not shown).

Electrophysiologic analysis

Chung *et al*. (2004) reported that 2-aminoethoxydiphenyl borate (2-APB) produces robust activation of recombinant TRPV3 in human embryonic kidney 293 cells and that 2-APB also sensitizes TRPV3 to activation by heat. In the light of these results, we examined the temperature response to primary keratinocytes expressing TRPV3 with and without the *Nh* mutation. A low concentration of 2-APB ($>100\,\mu$M) could not activate TRPV3 with or without the *Nh* mutation at room temperature (Figure S2), whereas a higher concentration of 2-APB could activate both kinds of keratinocytes. Primary keratinocytes expressing TRPV3 with or without the *Nh* mutation were incubated with fluorescence dye and 100 μM 2-APB at room temperature in a 96-microwell plate for 30 minutes. Next, we measured fluorescence from both keratinocytes after sequential thermal stimulation (Figure 7). Only keratinocytes from mice with the *Nh* mutation were activated by heat ($<33^{\circ}$C) in the presence of 100 μM 2-APB.

DISCUSSION

In this study, the use of a high-resolution genetic and physical mapping approach localized the *Nh* locus to a minimal genomic region of 1,000 kb, in which several genes were identified. Sequence analysis data indicated that only one nucleotide change was present in the coding region of the TRPV3 gene of DS-*Nh* mice, and that this was absent from other mouse strains examined in this study (BALB/c, C57BL/6, DBA, DS, NC/Nga, and NOD). This nucleotide change caused the substitution of Gly573 to Ser (*Nh* substitution) in TRPV3. Recently, we demonstrated that phenotypes resulting

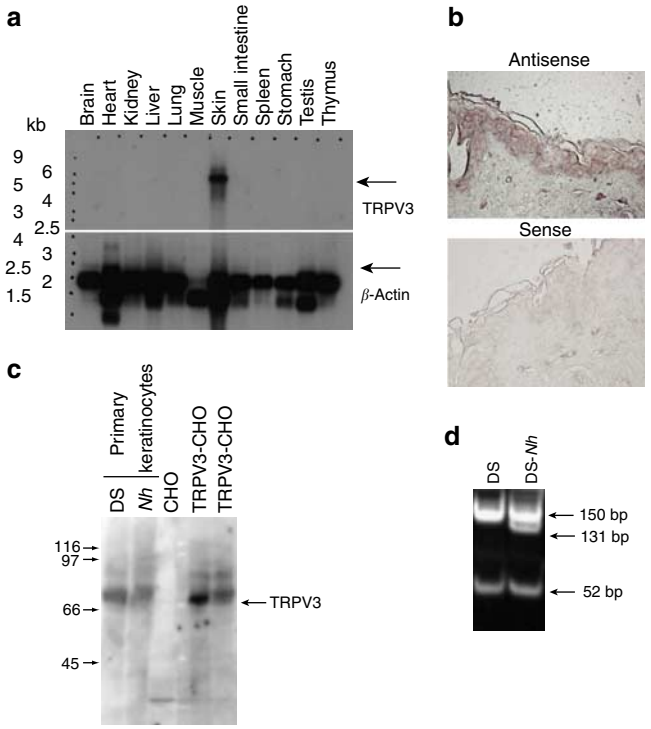

Figure 4. Detection of the TRPV3 gene and protein in DS-*Nh* mice. (**a**) Northern blot analysis was carried out in DS-*Nh* mice and showed the expression of TRPV3 (upper) or β-actin as a control (lower). TRPV3 is expressed in the skin region. (**b**) *In situ* hybridization study indicated that TRPV3 was expressed in skin keratinocytes in DS-*Nh* mice. Each panel shows a commonly observed image taken with an ×40 objective to illustrate an important area. (**c**) Keratinocytes from DS and DS-*Nh* mice were used in Western blot analysis and 20 μg of proteins was loaded in each lane. TRPV3-expressing CHO cells were used as a marker and 1–5 μg of proteins was loaded in each lane. The TRPV3 protein was detected in both strains. (**d**) RNA was extracted from skin, and used as template to check expression levels of mutated TRPV3 transcript by reverse transcription-PCR. PCR products were visualized by agarose gel electrophoresis.

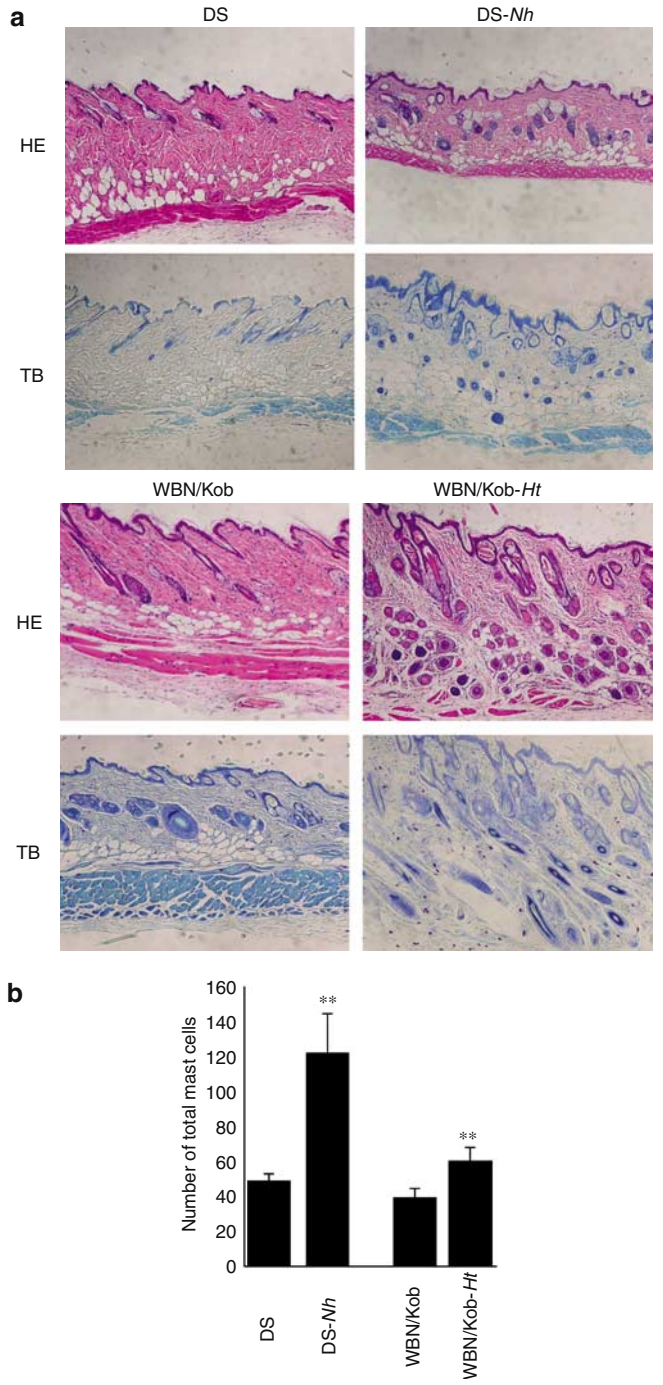

Figure 5. Histological characteristics of skin in DS, DS-*Nh*, WBN/Kob, and WBN/Kob-*Ht* strains at 5 weeks of age maintained in an SPF animal room. (**a**) Paraffin sections were stained with hematoxylin/eosin or toluidine blue. Each panel shows a commonly observed image taken with a ×10 objective to illustrate a wide area. (**b**) The numbers of mast cells per 2 mm of skin area in the skin tissue from DS and DS-*Nh* mice at 5 weeks of age were counted under a microscope with an eyepiece squared micrometer with a ×20 objective to provide a wide area. Each value represents the mean ± SD of five mice. Statistical significance was determined by the one-sided Student's *t*-test for unpaired two-group comparison. $^{**}P<0.01$ compared with age-matched DS mice or WBN/Kob rat.

from the hairless mutation of the WBN/Kob-*Ht* rat were morphologically and pathologically similar to those of the DS-*Nh* mouse (Asakawa *et al.*, 2005). The inheritance mode of the *Ht* mutation is autosomal dominant, and the *Ht* locus has been mapped to rat chromosome 10 (Akimoto *et al.*, 2000). As the rat TRPV3 gene was also mapped to rat chromosome 10, we sequenced its coding region, and detected one amino-acid alteration at the same position (Gly573 to Cys) as that in *TRPV3* of DS-*Nh* mice. These substitutions appear to result in hairlessness in these two rodents. Our breeding studies also suggested that both hairlessness and development of dermatitis were controlled by the *Nh* mutation, because observation of phenotypes of about 1,000 backcross progenies in the breeding study indicated that these two phenotypes did not segregate from each other. In addition, it is interesting that these characteristics of spontaneous dermatitis in both rodents were similar to human AD including the following: (1) *S. aureus* could be isolated from the skin lesions, (2) serum levels of IgE and IL-4 were significantly increased, (3) infiltration of inflammatory

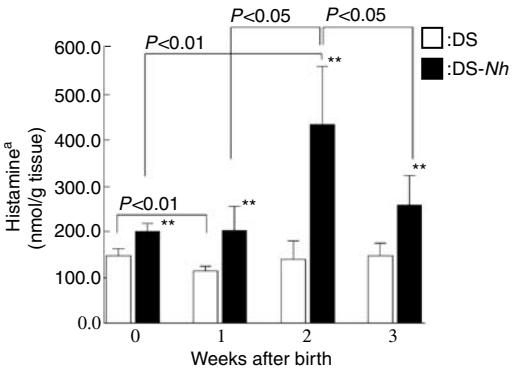

Figure 6. Histamine contents in the skin tissue from DS and DS-*Nh* mice maintained in an SPF animal room at 0, 1, 2, and 3 weeks of age. Each value represents the mean ± SD of five mice. Statistical significance was determined by the one-sided Student's *t*-test for unpaired two-group comparison. $^{**}P<0.01$ compared with age-matched DS mice. The levels of histamine in the skin from DS-*Nh* mice were significantly higher compared to those from age-matched DS mice.

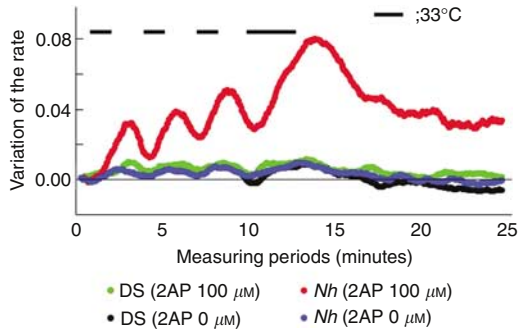

Figure 7. Heat activates TRPV3 in keratinocytes from DS and DS-*Nh* mice in the presence of 2-APB. We indicated that heat (>33°C) activated only mutated TRPV3 in keratinocytes from DS-*Nh* mice, using FDSS2000 microplate reader. The vertical axis of the figure indicates the variation ratio of fluorescence indicating the quantitative incorporation of Ca^{2+} into the cells. The horizontal axis indicates minutes after the start of the measurement. In this experiment, we used 100 μM 2-APB as the activator of TRPV3 because incorporation of Ca^{2+} did not occur at room temperature in this low concentration of 2-APB (Figure S1). We carried out at least five individual experiments using keratinocytes from each mouse and obtained the same results.

cells, and (4) hyperkeratosis was detected in skin lesions with dermatitis.

The Gly573Ser or Cys substitution in *TRPV3* was located near the pore region, and may cause reduction in flexibility in response to structural transformation for thermal stimulation, because Gly, a simple amino acid, was replaced with a more complicated one. In Figure 7, we indicated a lower temperature response to keratinocytes with the mutation compared to those without. Although it was clear that both TRPV3 and TRPV4 were expressed at keratinocytes, we considered that these responses were only caused through TRPV3 for the following two reasons. First, keratinocytes from both mice strains were not activated by heat (<33°C) in the absence of 2-APB, which is a selective TRPV3 activator at this concentration (Chung *et al.*, 2004). The other reason is that an increased response to sequential hot stimulations was indicated in our experiments, which is the remarkable trait in TRPV3 and TRPV1. The relationship between TRP and morphological changes is discussed in an interesting study (Di Palma *et al.*, 2002) – it was reported that a mutation in *Mcoln3* was associated with deafness in Va mice caused by morphological changes in hair cells in the organ of Corti. This amino-acid substitution of *Mcoln3* in these mice was located between the fourth and fifth transmembrane subunits, which is the site adjacent to the site of the *Nh* or *Ht* mutation in TRPV3. We thought that the gain of function in TRPV3 caused by a reduction of flexibility might evoke morphological changes involved in the hair loss in skin. In addition, Xu *et al.* (2002) reported that human TRPV3 was detected in cells surrounding hair follicles in human skin and Moqrich *et al.* (2005) reported that there is a hair irregularity in TRPV3-deficient mice. These reports indicate that TRPV3 plays some roles in normal hair growth through hyperfunctions.

DS-*Nh* mice and WBN/Kob-*Ht* rats showed larger numbers of mast cells at 5 weeks of age compared to their parent strains. However, mast cells do not appear to be essential for hair growth, because mast cell-deficient mice show normal hair growth. Several investigators have referred to the concept of a general role for mast cells in tissue remodeling (Irani *et al.*, 1992; Levi-Schaffer, 1995; Kendall *et al.*, 1997), and have strongly suggested that mast cells are involved in the control of mouse hair growth (Maurer *et al.*, 1997). For example, Asebia mice appear almost hairless, and show a significantly increased number of dermal mast cells (Brown and Hardy, 1988; Sundberg, 1994). In addition, numbers of mast cells in the skin of *hr*/*hr* and *nu*/*nu* mice were increased compared to that in BALB/c mice (Keller *et al.*, 1976; Sundberg, 1994). Furthermore, there are clinical indications that mast cells may be involved in the pathogenesis of a certain type of hair loss in humans (Lattanand and Johnson, 1975; Fiedler and Alaiti, 1996; Xu *et al.*, 2003).

Just before anagenesis starts, histamine level in the skin lesion increases transiently, and then returns to normal level by which time hair growth begins (Hamada and Suzuki, 1996). In fact, histamine levels in the skin from DS mice at 0 weeks of age increases transiently compared to those from DS mice at 1, 2, and 3 weeks of age (Figure 6). We think that this increase may be important for developing normal hair growth after birth in mice. On the other hand, larger amounts of histamine were detected in the skin of DS-*Nh* mice at 0, 1, 2, and 3 weeks of age compared to those from age-matched DS mice (Figure 6). Furthermore, we could not detect a transient increase in the level of histamine in the skin from DS-*Nh* mice at 0 weeks of age (Figure 6). Maintenance of these higher levels of histamine may cause hairlessness in DS-*Nh* mice. From the point of view of AD-like dermatitis, Hossen *et al.* (2005) reported that an increase in histamine in skin lesions could evoke an AD-like symptom via scratching behavior in HR-1 mice on a low-magnesium diet, which is similar to spontaneous dermatitis in DS-*Nh* mice. Although the increase in histamine levels in DS-*Nh* mice is caused by an as yet unknown mechanism, histamine could induce

keratinocytes to produce nerve growth factor (NGF) via H1 receptors (Kanda and Watanabe, 2004). Recently, some investigators suggested that NGF plays an important role in the development of AD (Toyoda *et al.*, 2002) or AD-like symptoms (Tanaka and Matsuda, 2005). Interestingly, Gopinath *et al.* (2005) speculated that increased expression of *TRPV3* might affect the production of NGF in keratinocytes. Furthermore, levels of serum and skin NGF significantly increased only in DS-*Nh* mice with AD-like dermatitis, and not in DS-*Nh* mice without dermatitis (Yoshioka *et al.*, 2006) and DS mice (data not shown). Levels of NGF in DS-*Nh* mice were reduced by H-1 antagonist through inhibition of NGF production from keratinocytes, and this reduction should improve skin lesions associated with AD-like dermatitis (Yoshioka *et al.*, 2006). From the role and involvement of NGF in hairlessness, it is clear that a higher concentration of NGF at the skin plays an important role in control of the hair growth cycle via mechanisms of anagen rising or anagen maintaining (Peters *et al.*, 2006), whereas a prolonged anagen phase was associated with hairlessness in mice (Prowse *et al.*, 1999). We showed hair follicles from rodents with wild-type and mutated TRPV3 at the same age in Figure 5a. Our data indicated that follicles from mutated rodents were in anagen, whereas those from wild rodents were not. Taken together, we speculated that gain of function in mutated TRPV3 was associated with an abnormal hair growth cycle through the production of NGF caused by a higher concentration of histamine in the skin and that this prolonged the anagen phase causing hairlessness.

Little is known about the *in vivo* roles of TRPV3. In this study, we reported for the first time that hyperergasia of TRPV3 caused hairlessness and might be associated with the development of AD-like dermatitis in rodents via an increase in the number of mast cells. Thus, TRPV3 has the potential to become a therapeutic target for human hair loss and AD.

MATERIALS AND METHODS

Animals

All mice used in this study were maintained in microisolator cages, exposed to a 12 hours light/12 hours dark cycle, and provided with standard food and water *ad libitum*. Animals were housed in rooms, under SPF conditions or conventional conditions. This study was conducted according to the guidelines for animal experimentation at Shionogi & Co., Ltd.

Breeding studies

DS-*Nh* (*Nh*/*Nh*) mice were crossed with DS, BALB/c, or C57BL/6 mice (N1 generation). F1 progenies with the hairless mutation were backcrossed with BALB/c or C57BL/6 mice, to produce the first backcross generation (N2) mice. We kept about 1,000 N1 and N2 progenies under conventional conditions, and confirmed the development of dermatitis.

Positional cloning of the candidate gene using polymorphic DNA markers and BAC libraries

DS-*Nh* (Nh/+) mice were crossed initially with NC/Nga mice. F1 progenies (Nh/+) were backcrossed with NC/Nga mice to produce the first backcross generation (N2). A total of 2,303 backcross progenies were categorized into non-hair and haired mice by phenotype, and then genomic DNA samples were prepared from the liver or tail end and used for linkage analysis. Microsatellite markers were purchased from Research Genetics/Invitrogen (San Diego, CA). Simple sequence length polymorphisms (PCR-SSLP) were analyzed: 1 μl (100 ng) genomic DNA was amplified in a total volume of 15 μl with final concentrations of 1 × Gold buffer II, 1.5 mM $MgCl_2$, 200 μM dNTPs, 0.25 μM of each primer, and 0.1 U AmpliTaq Gold polymerase (Applied Biosystems, Foster City, CA). Reactions were carried out in a DNA Engine thermal cycler (MJ Research, Waltham, MA), with a PCR profile of one cycle at 95°C for 5 minutes, and 40 cycles of 94°C for 30 seconds, 55°C for 40 seconds, and 72°C for 60 seconds. PCR products were loaded on 4% agarose gels (3% NuServe agarose and 1% agarose).

We constructed BAC libraries of DS and DS-*Nh* mice for genomic sequencing. The libraries were screened using PCR, and BAC clones including the *Nh* region were picked up. After the BAC clone cultures were lysed using the alkaline lysate method, the harvested DNA was sheared by nebulizing at 8 psi, and the resulting fragments were end-repaired and subcloned into pUC18 vectors. Following transformation into *E. coli* XL1 Blue cells, plasmid DNAs were isolated using an automated alkaline lysate method, and were end-sequenced using the ABI BigDye version 3 Prism sequencing kit. Products of the cycle sequencing reaction were resolved, and detected using Perkin-Elmer ABI 9600 sequencers.

Detection of TRPV3 gene and protein

Mouse RNAs from various tissues were extracted and electrophoresed on agarose gels, then transferred to nylon membranes. A TRPV3-specific probe was obtained by PCR-based amplification of a mouse skin cDNA library using a biotinylated primer having the same sequence as mouse TRPV3. The biotinylated probe hybridized against immobilized RNA was used to detect TRPV3 mRNA.

Tissue sections (10 μm) from DS-*Nh* mice were fixed in a 4% phosphate-buffered saline-buffered paraformaldehyde solution for 30 minutes, permeated in 0.3% Triton X-100 in phosphate-buffered saline, post-fixed in a 4% phosphate-buffered saline-buffered paraformaldehyde solution, and digested with 2 μg/ml proteinase K for 7.5 minutes at 37°C. Prehybridization was carried out for 30 minutes at room temperature in 4 × SSC (sodium saline citrate; 0.15 M NaCl, 0.015 M sodium citrate, pH 7.4) containing 50% formamide. Next, hybridization was performed at 37°C for 16 hours in a hybridization solution containing 10 mM Tris-HCl, pH 7.4, 50% formamide, 4 × SSC, 10% dextran sulfate, 125 μg/ml salmon sperm DNA, 250 μg/ml yeast tRNA, 0.02% SDS, and 100 nM Dig-labeled TRPV3 probe. Antisense and sense primers were prepared from linearized plasmid vectors containing the mouse TRPV3 sequence, using RNA polymerase. Here, plasmid vectors containing the polymerase from bacteriophages T7 (for sense) and SP6 (antisense) were used. Following hybridization, tissue sections were incubated with anti-Dig (Fab), conjugated with alkaline phosphatase (Boehringer Mannheim, Mannheim, Germany), and color development was performed at 25°C in a buffer containing *p*-nitroblue tetrazolium chloride and 5-bromo-4-chloro-3-indolyphosphate (Boehringer Mannheim, Germany) for 16–20 hours.

Primary mouse keratinocytes from DS and DS-*Nh* mice and TRPV3-expressing CHO cells were lysed, filtered, and blotted under non-reducing conditions using 10% SDS-PAGE. Polypeptides

(VRL3-1; RTTAPGGNPVVLTEKC) having the same sequence as mouse TRPV3 were immunized in rabbits to obtain polyclonal antibodies against mouse TRPV3. This polyclonal antibody was used to detect TRPV3 proteins.

Crude RNAs were extracted from primary keratinocytes and 1 μg total RNA was converted to double-stranded cDNA. Two rounds of TRPV3 gene-specific PCR were performed to estimate the expressing ratio. First PCRs were performed to amplify gene segment containing the *Nh* mutation using this cDNA as a template and the primers listed in Figure S1. Second PCRs were performed to implement the *Alu*I recognition site in PCR products with the *Nh* mutation. Each of the PCR products was digested with *Alu*I, and the estimation of expression ratio determined by the restriction fragment length polymorphism band pattern on a 4% agarose gel.

Histopathological analysis of DS-*Nh* and DS mice

Paraffin sections were prepared from the skin, lungs, and intestines from DS and DS-*Nh* mice at 5 weeks of age, and were stained with acidic toluidine blue to count the number of mast cells.

Measurement of histamine levels in skin tissues

Skin tissues from DS and DS-*Nh* mice at 0, 1, 2, and 3 weeks of age were collected, homogenized, and stored at 80°C until measurement of histamine. After the homogenates were boiled for 10 minutes and centrifuged at 12,000 r.p.m., supernatants were used to measure histamine levels using an enzyme-linked color developing kit (Kikkoman, Chiba, Japan). Procedures were according to the manufacturer's instructions, except for the volume and the dilution of the skin tissue samples.

Measurement of intracellular Ca^{2+} mobilization

We carried out measurements of Ca^{2+} influx into keratinocytes from DS and DS-*Nh* mice by *Nh*-mutated and wild-type TRPV3 after sequential thermal stimulation. Keratinocytes from DS and DS-*Nh* mouse were seeded into 96-well assay plates. Cells were immediately loaded for 30 minutes with 4 μM Fura2-AM or Fluo3-AM (Invitrogen) in Hank's balanced salt buffer at 25°C containing 100 μM 2-APB (room temperature) and the fluorescence dyes washed out by Hank's balanced salt buffer. Cells loaded with Fluo3-AM were treated with different concentrations of 2-APB after 100 μl of Hank's balanced salt buffer supplementation and then their fluorescence was detected by an FDSS3000 (Hamamatsu Photonics KK, Hamamatsu, Japan) (Figure S2). Further, cells loaded with Fura2-AM were treated with repeating thermal stimulation after 20 μl of Hank's balanced salt buffer supplementation and their fluorescence was detected by an FDSS2000 (Hamamatsu Photonics KK) (Figure 7).

CONFLICT OF INTEREST

The authors state no conflict of interest.

ACKNOWLEDGMENTS

We thank Dr Yukihiko Kitamura for guidance and valuable discussion.

SUPPLEMENTARY MATERIAL

Figure S1. A gene fragment of TRPV3 with the *Nh* mutation and sequences of oligonucleotides used for PCR in this study.

Figure S2. Experimental determination of 2-APB concentration for our experiment.

REFERENCES

Akimoto T, Suzuki H, Nakama K, Suzuki K (2000) Locus of dominant hairless gene (*Ht*) causing abnormal hair and keratinization maps to rat chromosome 10. *Exp Anim* 49:137–40

Asakawa M, Yoshioka T, Hikita I, Matsutani T, Hirasawa T, Arimura A *et al.* (2005) WBN/Kob-*Ht* rats spontaneously develop dermatitis under conventional conditions: another possible model for atopic dermatitis. *Exp Anim* 54:461–5

Brown WR, Hardy MH (1988) A hypothesis on the cause of chronic epidermal hyperproliferation in asebia mice. *Clin Exp Dermatol* 13: 74–7

Chung MK, Lee H, Mizuno A, Suzuki M, Caterina MJ (2004) 2-Aminoethoxydiphenyl borate activates and sensitizes the heat-gated ion channel TRPV3. *J Neurosci* 24:5177–82

Di Palma F, Belyantseva IA, Kim HJ, Vogt TF, Kachar B, Noben-Trauth K (2002) Mutations in Mcoln3 associated with deafness and pigmentation defects in varitint-waddler (Va) mice. *Proc Natl Acad Sci USA* 99:14994–9

Enerback L, Wingren U (1980) Histamine content of peritoneal and tissue mast cells of growing rats. *Histochemistry* 66:113–24

Fiedler VC, Alaiti S (1996) Treatment of alopecia areata. *Dermatol Clin* 14:733–7

Galli SJ, Nakae S, Tsai M (2005) Mast cells in the development of adaptive immune responses. *Nat Immunol* 6:135–6142

Gopinath P, Wan E, Holdcroft A, Facer P, Davis JB, Smith GD *et al.* (2005) Increased capsaicin receptor TRPV1 in skin nerve fibres and related vanilloid receptors TRPV3 and TRPV4 in keratinocytes in human breast pain. *BMC Womens Health* 5:4–9

Hamada K, Suzuki K (1996) Evaluation of biochemical indices as a hair cycle marker in C3H mice. *Exp Anim* 45:251–6

Haraguchi M, Hino M, Tanaka H, Maru M (1997) Naturally occurring dermatitis associated with *Staphylococcus aureus* in DS-*Nh* mice. *Exp Anim* 46:225–9

Hikita I, Yoshioka T, Mizoguchi T, Tsukahara K, Tsuru K, Nagai H *et al.* (2002) Characterization of dermatitis arising spontaneously in DS-*Nh* mice maintained under conventional conditions: another possible model for atopic dermatitis. *J Dermatol Sci* 30:142–53

Hossen MA, Fujii Y, Ogawa M, Takubo M, Tsumuro T, Kamei C (2005) Effect of loratadine on mouse models of atopic dermatitis associated pruritus. *Int Immunopharmacol* 5:1331–6

Irani AM, Gruber BL, Kaufman LD, Kahaleh MB, Schwartz LB (1992) Mast cell changes in scleroderma. Presence of MCT cells in the skin and evidence of mast cell activation. *Arthritis Rheum* 35:933–9

Kanda N, Watanabe S (2004) Histamine enhances the production of granulocyte–macrophage colony-stimulating factor via protein kinase C alpha and extracellular signal-regulated kinase in human keratinocytes. *J Invest Dermatol* 122:863–72

Keller R, Hess MW, Riley JF (1976) Mast cells in the skin of normal, hairless and athymic mice. *Experientia* 32:171–2

Kendall JC, Li XH, Galli SJ, Gordon JR (1997) Promotion of mouse fibroblast proliferation by IgE-dependent activation of mouse mast cells: role for mast cell tumor necrosis factor-alpha and transforming growth factor-beta 1. *J Allergy Clin Immunol* 99:113–23

Lattanand A, Johnson WC (1975) Male pattern alopecia: a histopathologic and histochemical study. *J Cutan Pathol* 2:58–70

Levi-Schaffer F (1995) Mast cell/fibroblast interactions in health and disease. *Chem Immunol* 61:161–85

Maurer M, Fischer E, Handjiski B, von Stebut E, Algermissen B, Bavandi A (1997) Activated skin mast cells are involved in murine hair follicle regression (catagen). *Lab Invest* 77:319–32

Mitchell EB, Crow J, Williams G, Platts-Mills TA (1986) Increase in skin mast cells following chronic house dust mite exposure. *Br J Dermatol* 114:65–73

Moqrich A, Hwang SW, Earley TJ, Petrus MJ, Murray AN, Spencer KS (2005) Impaired thermosensation in mice lacking TRPV3, a heat and camphor sensor in the skin. *Science* 307:1468–72

Peters EM, Hendrix S, Golz G, Klapp BF, Arck PC, Paus R (2006) Nerve growth factor and its precursor differentially regulate hair cycle progression in mice. *J Histochem Cytochem* 54:275–88

Piloto Valdes L, Gomez Echevarria AH, Valdes Sanchez AF, Ochoa Ochoa C, Chong Lopez A, Mier Naranjo G (1990) Atopic dermatitis. Findings of skin biopsies. *Allergol Immunopathol* 18:321–4

Prowse DM, Lee D, Weiner L, Jiang N, Magro CM, Baden HP *et al.* (1999) Ectopic expression of the *nude* gene induces hyperproliferation and defects in differentiation: implications for the self-renewal of cutaneous epithelia. *Dev Biol* 212:54–67

Sundberg JP (1994) *Handbook of mouse mutations with skin and hair abnormalities; animal models and biomedical tools*. New York: CRC Press

Tanaka A, Matsuda H (2005) Expression of nerve growth factor in itchy skins of atopic NC/NgaTnd mice. *J Vet Med Sci* 67:915–9

Toyoda M, Nakamura M, Makino T, Hino T, Kagoura M, Morohashi M (2002) Nerve growth factor and substance P are useful plasma markers of disease activity in atopic dermatitis. *Br J Dermatol* 147:71–9

Watanabe A, Takeuchi M, Nagata M, Nakamura K, Nakao H, Yamashita H *et al.* (2003) Role of the *Nh* (Non-hair) mutation in the development of dermatitis and hyperproduction of IgE in DS-*Nh* mice. *Exp Anim* 52:419–23

Weber S, Kruger-Krasagakes S, Grabbe J, Zuberbier T, Czarnetzki BM (1995) Mast cells. *Int J Dermatol* 34:1–10

Xu H, Ramsey IS, Kotecha SA, Moran MM, Chong JA, Lawson D *et al.* (2002) TRPV3 is a calcium-permeable temperature-sensitive cation channel. *Nature* 418:181–6

Xu X, Solky B, Elenitsas R (2003) Scarring alopecia associated with mastocytosis. *J Cutan Pathol* 30:561–5

Yoshioka T, Hikita I, Matsutani T, Yoshida R, Asakawa M, Toyosaki-Maeda T *et al.* (2003) DS-*Nh* as an experimental model of atopic dermatitis induced by *Staphylococcus aureus* producing staphylococcal enterotoxin C. *Immunology* 108:562–9

Yoshioka T, Hikita I, Asakawa M, Hirasawa T, Deguchi M, Matsutani T *et al.* (2006) Spontaneous scratching behavior in DS-*Nh* mice as a possible model for pruritus in atopic dermatitis. *Immunology* 118:293–301

Zhang JI, Fang SG, Wang CY (2005) A novel nonsense mutation and polymorphisms in the mouse hairless gene. *J Invest Dermatol* 124: 1200–5